Journal of ELECTRICAL ENGINEERING, VOL 70 (2019), NO-7S, 1–15

sciendo

PAPERS

Temperature dependent dispersion models applicable in solid state physics

Daniel Franta, Jiří Vohánka, Martin Čermák, Pavel Franta, Ivan Ohlídal*

Dispersion models are necessary for precise determination of the dielectric response of materials used in optical and microelectronics industry. Although the study of the dielectric response is often limited only to the dependence of the optical constants on frequency, it is also important to consider its dependence on other quantities characterizing the state of the system. One of the most important quantities determining the state of the condensed matter in equilibrium is temperature. Introducing temperature dependence into dispersion models is quite challenging. A physically correct model of dielectric response must respect three fundamental and one supplementary conditions imposed on the dielectric function. The three fundamental conditions are the time-reversal symmetry, Kramers-Kronig consistency and sum rule. These three fundamental conditions are valid for any material in any state. For systems in equilibrium there is also a supplementary dissipative condition. In this contribution it will be shown how these conditions can be applied in the construction of temperature dependent dispersion models. Practical results will be demonstrated on the temperature dependent dispersion model of crystalline silicon.

K e y w o r d s: temperature dependent dielectrics dispersion model, Kramers-Kronig relation, crystalline silicon

1 Introduction

Dispersion models describe the linear dielectric response. In the case of isotropic materials without spatial dispersion the dielectric response is usually described by the *dielectric function* $\hat{\varepsilon}(\omega)$ expressing the linear relation between the electric field $\hat{\boldsymbol{E}}(\omega, \hat{\boldsymbol{k}})$ and the electric displacement field $\hat{\boldsymbol{D}}(\omega, \hat{\boldsymbol{k}})$

$$\hat{\boldsymbol{D}}(\omega, \hat{\boldsymbol{k}}) = \epsilon_0 \, \hat{\varepsilon}(\omega) \, \hat{\boldsymbol{E}}(\omega, \hat{\boldsymbol{k}}), \tag{1}$$

where ϵ_0 is the permittivity of vacuum, ω is frequency and $\hat{\boldsymbol{k}}$ is the complex wavevector.

The complex dielectric function must fulfill three fundamental conditions [1-4]: the *time-reversal symmetry*

$$\hat{\varepsilon}(\omega) = \hat{\varepsilon}^*(-\omega), \tag{2}$$

the *Kramers-Kronig consistency*

$$\varepsilon_\mathrm{r}(\omega) = 1 + \frac{1}{\pi} \int_{-\infty}^{\infty} \frac{\varepsilon_\mathrm{i}(\xi)}{\xi - \omega} \, \mathrm{d}\xi \tag{3}$$

and the *sum rule*

$$\int_0^\infty \omega \, \varepsilon_\mathrm{i}(\omega) \, \mathrm{d}\omega = \frac{\pi}{2} \omega_\mathrm{p}^2 , \tag{4}$$

where ω_p is a constant called the plasma frequency. The first two conditions can be merged into one equation

$$\varepsilon_\mathrm{r}(\omega) = 1 + \frac{2}{\pi} \int_0^\infty \frac{\xi \, \varepsilon_\mathrm{i}(\xi)}{\xi^2 - \omega^2} \mathrm{d}\xi. \tag{5}$$

These conditions express the fact that if the dielectric response is described using the susceptibility function in the time domain, then this function is a real causal function. The third condition is a result of the combination of the superconvergence theorem and the asymptotic behavior of any dielectric response, *ie* that for high frequencies all dispersion models converge to the model of *sparse plasma*. The sum rule condition is important for the construction of dispersion models because it expresses the relation between the integral value of the quantity $\omega\varepsilon_\mathrm{i}(\omega)$ and the density of electrons $\mathcal{N}_\mathrm{e}$ and nuclei $\mathcal{N}_n$ in the material [5-7]

$$\omega_\mathrm{p}^2 = \frac{e^2 \mathcal{N}_\mathrm{e}}{\epsilon_0 m_\mathrm{e}} + \sum_n \frac{e^2 Z_n^2 \mathcal{N}_n}{\epsilon_0 m_n}, \tag{6}$$

where e is the elementary charge and m_e is the electron mass. The symbols Z_n and m_n denote the proton number and mass of nuclei of type n.

In addition to the three fundamental conditions, which hold for the system in any state, there is one additional supplementary condition fulfilled for systems in thermodynamic equilibrium. This supplementary *dissipative condition* expresses the fact that for systems in equilibrium

*Department of Physical Electronics, Faculty of Science, Masaryk University, Kotlářská 2, 611 37 Brno, Czechia, franta@physics.muni.cz

DOI: 10.2478/jee-2019–0036, Print (till 2015) ISSN 1335-3632, On-line ISSN 1339-309X

© This is an open access article licensed under the Creative Commons Attribution-NonCommercial-NoDerivs License (http://creativecommons.org/licenses/by-nc-nd/3.0/).

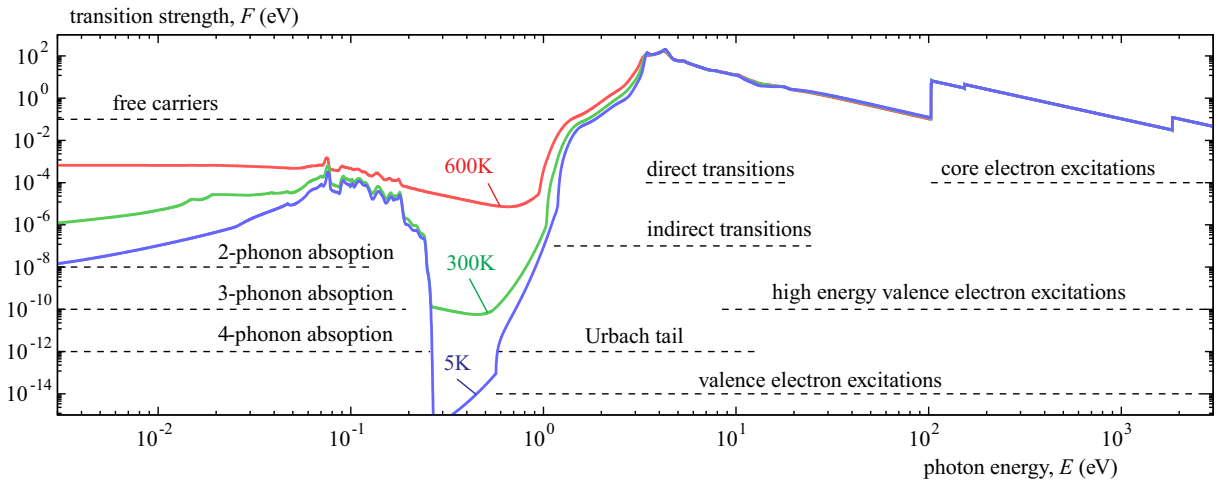

Fig. 1. Transition strength function $F(E,T)$ of c-Si calculated using our model in the spectral range covering all the optical excitations for three selected temperatures

the absorption processes are more probable than the stimulated emission processes

$$\varepsilon_{\mathrm{i}}(\omega) \geq 0 \quad \text{for} \quad \omega > 0\,. \tag{7}$$

For the description of dispersion models it is more common to use the photon energy $E = \hbar\omega$ ($\hbar$ is the reduced Planck's constant) instead of frequency ω. Moreover, it is convenient to describe the dielectric response using the function $F(E,T) = E\varepsilon_{\mathrm{i}}(E,T)$ which is in our nomenclature called the *transition strength function*. Note that in order to emphasize that the dielectric response is temperature dependent, we explicitly indicated the dependence on temperature T. The equations(4), (5) and (6) can be rewritten as [6, 7]

$$\varepsilon_{\mathrm{r}}(E,T) = 1 + \frac{2}{\pi}\int_0^\infty \frac{F(X,T)}{X^2 - E^2}\,\mathrm{d}X\,, \tag{8}$$

$$\varepsilon_{\mathrm{i}}(E,T) = \frac{F(E,T)}{E}\,, \tag{9}$$

$$\int_0^\infty F(E,T)\,\mathrm{d}E = N(T)\,, \tag{10}$$

$$N(T) = \frac{\pi e^2\hbar^2\mathcal{N}_{\mathrm{e}}(T)}{2\epsilon_0 m_{\mathrm{e}}} + \sum_n \frac{\pi e^2 Z_n^2\hbar^2\mathcal{N}_n(T)}{2\epsilon_0 m_n}\,, \tag{11}$$

where the quantity $N(T)$ is called the *total transition strength* or just *transition strength*. It should be noted that according to (10) the transition strength function $F(E,T)$ could be interpreted as a non-negative distribution function for the total transition strength $N(T)$. The example of the transition strength function is in Fig. 1, where the horizontal bars indicate the spectral ranges of the individual elementary excitations.

Equations (8), (9), (10) and (11) form a basis for the construction of our dispersion models [6-8]. In order to describe the concrete materials, it necessary to perform one more step. It is necessary to separate the total transition strength into terms corresponding to individual elementary excitation

$$F(E,T) = \sum_t N_t(T) F_t^0(E,T)\,, \tag{12}$$

where the index t distinguishes the individual elementary excitations, and the functions $F_t^0(E,T)$, called the *normalized transition strength functions of elementary excitations*, are normalized to unity with respect to the sum rule integral

$$\int_0^\infty F_t^0(E,T)\,\mathrm{d}E = 1\,. \tag{13}$$

The quantities $N_t(T)$ are called the *transition strengths of elementary excitations* and their sum gives the total transition strength

$$\sum_t N_t(T) = N(T)\,. \tag{14}$$

The elementary excitations are, for example, direct or indirect electronic excitations, one branch of two-phonon absorption, *etc* (see fig Fig. 1). The number of the contributions depends on the specific material and also on the required accuracy of the dispersion model. For example, for amorphous materials it is not necessary to model the direct and indirect electronic transitions separately because these transitions are indistinguishable in such materials, therefore, it is possible to model them by one contribution. While it is not necessary to model the multi-phonon excitations in the dispersion model used for very thin films because they are weak, it is necessary to take the multi-phonon absorption processes into account in the dispersion model used for the thick slab.

The ideas presented in this work are applicable to a wide range of materials. Their concrete utilization will be discussed in the context of the temperature dependent dispersion model of crystalline silicon [9-12].

2 Thermal expansion effect

The total transition strength $N(T)$ depends on the density of the charged particles in the system, therefore, if the number of the particles is constant, then the transition strength is inverse proportional to the volume of the system $V(T)$

$$N(T) = N^{300\mathrm{K}} \frac{V(T_\mathrm{R})}{V(T)}\,, \tag{15}$$

where $N^{300\mathrm{K}}$ is the transition strength at the *reference temperature* T_R and $V(T_\mathrm{R})$ is the volume at this temperature. In our work we define the reference temperature (RT) in the value of 300 K. Since the temperature in our laboratory is kept at this value, the abbreviation RT can be also interpreted as the room temperature. Note that this temperature is different from 293.15 K (20 °C) defined in ISO 1 as the room temperature [13]. If the density of the charged particles in the system is known, *eg* for the crystalline silicon (c-Si), then the value of $N^{300\mathrm{K}}$ can be expressed using (11). For the crystalline silicon the total transition strength at the reference temperature is $N^{300\mathrm{K}} = 1515\ \mathrm{e}V^2$ [6]. In other cases the density of the charged particles may not be known and the value of $N^{300\mathrm{K}}$ must be interpreted as a free parameter of the dispersion model. In real situations the knowledge of the exact value of $N^{300\mathrm{K}}$ is not necessary for the construction of the dispersion model because this value corresponds to the value calculated by the sum rule integral over the whole spectral range covering also the spectral range of high energies, which is not experimentally accessible using the table-top instruments. On the other hand, the expansion factor is very important for the construction of the temperature dependent dispersion model because the relative changes of the optical constants affect the interference effects in thin film systems and thick slabs.

For the proper interpretation of the interference effects in the data measured at different temperatures, it is also necessary to know the temperature dependencies of the thicknesses in the system under study. Of course, the temperature dependencies of the volume and thicknesses are correlated effect. They can be described using the quantity called the *linear thermal expansion*, which is for the isotropic materials given by the scalar function $e(T)$ defined as follows

$$e(T) = \frac{L(T) - L(T_\mathrm{R})}{L(T_\mathrm{R})}\,, \tag{16}$$

where $L(T)$ is the linear dimension of the system at temperature T. The total transition strength and the thickness of the film or slab is then calculated from the values at the reference temperature as

$$N(T) = N^{300\mathrm{K}}\, \mathcal{E}(T)\,, \tag{17}$$

where $\mathcal{E}(T)$ is the *expansion factor* defined as

$$\mathcal{E}(T) = \frac{V(T_\mathrm{R})}{V(T)} = \left[\frac{1}{1+e(T)}\right]^3 \tag{18}$$

and

$$d(T) = d^{300\mathrm{K}}\left[1 + e(T)\right]\,, \tag{19}$$

where $d^{300\mathrm{K}}$ is the thickness at the reference temperature. In our software [14] the model of the linear thermal expansion is implemented as a part of the dispersion model and it is used not only to calculate the changes in the total transition strength but also to calculate the changes in the thicknesses.

In the frame of the quasiparticle approximation the linear thermal expansion depends linearly on the phonon occupation numbers. Therefore it can be calculated by means of the integration over the Brillouin zone. As it was shown in [12, 15, 16], the temperature dependence of the linear thermal expansion can be modeled using the *average Bose–Einstein statistical factors* (ABESF). In this model the continuous distribution of phonons is represented by a small number of average phonons, and the linear thermal expansion is given as follows

$$e(T) = e_0 + \sum_j \frac{e_j}{\exp(\Theta_j/T) - 1}\,, \tag{20}$$

where the index j distinguishes the terms corresponding to the individual average phonons, e_0 is the value of $e(0\,\mathrm{K})$, Θ_j are the energies of the average phonons expressed as temperatures and e_j control the magnitudes of the individual ABESF terms. The value e_0 is dependent on the other parameters e_j, Θ_j and it can be calculated from the condition $e(T_\mathrm{R}) = 0$ as follows

$$e_0 = -\sum_j \frac{e_j}{\exp(\Theta_j/T_\mathrm{R}) - 1} \tag{21}$$

The linear thermal expansion usually increases with the increasing temperature, but for many materials there are certain temperature ranges (usually for low temperatures) in which this function decreases. This effect is called the anomalous thermal expansion. The anomalous thermal expansion at low temperatures is exhibited by common materials such as H_2O (ice up to 70 K [17]) or SiO_2 (fused silica up to 150 – 190 K [18]). The materials with the anomalous thermal expansion at high temperatures are, for example, ZrW_2O_8 (up to 1050 K [19]) or ScF_3 (up to 1100 K [20]).

The linear thermal expansion of c-Si has been measured with high accuracy for below the room temperatures in the recently published work of Middelmann *et al* [16]. The updated version of the dispersion model of c-Si uses the formula of linear thermal expansion based on these data and Watanabe *et al* data. The column named "1-st fit" shows the parameters in the three-term formula obtained by fitting the raw measured data of the temperature dependence of the length $L(T)$ of sample 2, which were kindly provided by the colleagues from the German metrology institute PTB. These values are in a

Table 1. Values of the parameters of the linear thermal expansion models obtained by fitting the Middelmann *et al* [16], Watanabe *et al* [21] and Ibach's [15] experimental data

parameter	4-th fit in [12]	1-st fit	2-nd fit	3-rd fit
e_1	-0.00017(2)	-0.0001946(10)	-0.0001865(8)	-0.0001947(13)
e_2	0.00332(3)	0.00262(8)	0.003077(12)	0.00262(9)
e_3	0.00186(12)	0.00089(7)	0.000631(8)	0.00088(8)
e_4	–	–	–	0.0023(3)
Θ_1 (K)	198(9)	199.6(3)	197.1(3)	199.6(4)
Θ_2 (K)	652(6)	612(3)	633.5(8)	612(4)
Θ_3 (K)	3033(133)	893(23)	1249(17)	894(24)
Θ_4 (K)	–	–	–	3721(141)
χ (fit quality)				
e Watanabe *et al*	0.275	–	1.231	0.372
α Watanabe *et al*	0.115	–	–	–
α Ibach	0.257	–	–	–
L Middelmann *et al*	–	0.561	0.662	0.561

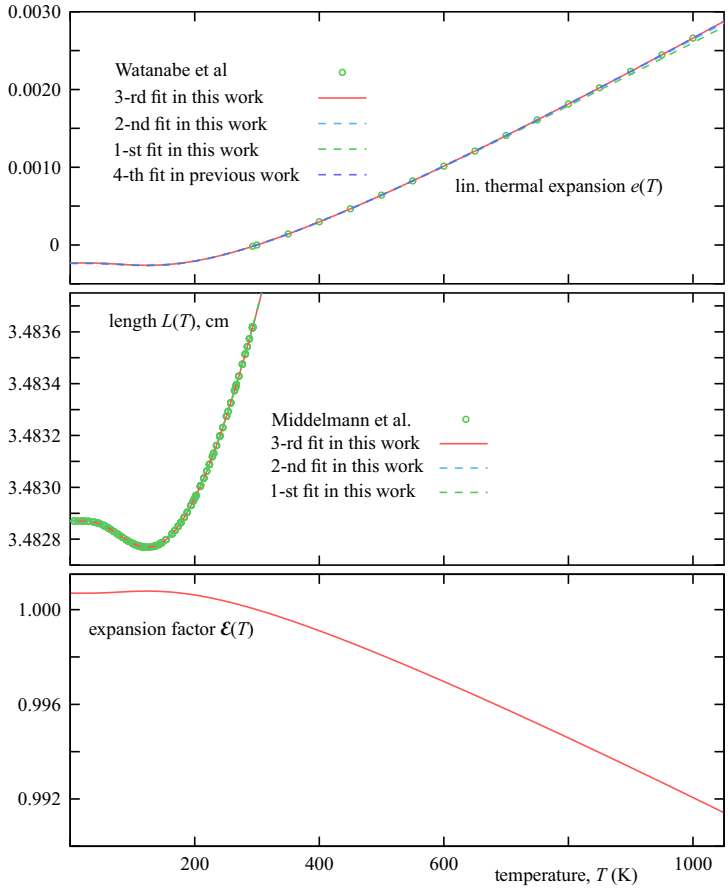

Fig. 2. Temperature dependencies of the linear thermal expansion $e(T)$ and expansion factor $\mathcal{E}(T)$ of c-Si

good agreement with the fit presented in Middelmann *et al* work. The column named "2-nd fit" corresponds to the three-parameter formula fitted on both the Middelmann *et al* and Watanabe *et al* data. From the values of the quantity χ describing the quality of the fit it is evident that the obtained fit is worse than the fits in the first two columns. This is especially true for the fit of the Watanabe *et al* data ($\chi = 0.275$ for the 4-th fit in [12] and $\chi = 1.231$ for the 2-nd fit). For this reason we added the fourth ABESF term in to the formula (20). The parameters corresponding to this fit are in the last column named "3-rd fit". Considering more than four ABESF terms did not result in better fit of the experimental data. The Watanabe *et al* and Middelmann *et al* experimental

data and their fits are depicted in Fig. 2. The experimental data for $e(T)$ are taken from Watanabe *et al* work [21]. The quantity $L(T)$ is the length of sample 2 in the Middelmann *et al* work [16]. Note that the curves are almost identical, small differences are visible only at high temperatures. The values calculated using the formula corresponding to the 1-st fit do not describe the experimental data at high temperatures very well. This is not surprising since the Watanabe *et al* data were not used for this fit. The negative value of e_1 corresponds to the anomalous thermal expansion in the region below 125 K (see course of $L(T)$ in Fig. 2). The temperature dependence of the expansion factor $\mathcal{E}(T)$ used in our advanced dispersion model of c-Si, which is calculated using (18), is also plotted in Fig. 2.

The frequencies of the average phonons corresponding to temperatures Θ_1 and Θ_2 were 4.2 and 12.8 THz, respectively, which corresponds to the mean frequencies of the transversal acoustical and longitudinal or transversal optical phonons [10, 15]. While the longitudinal and transversal optical phonons contribute positively to the derivatives of the linear thermal expansion $e(T)$, the acoustical phonons contribute negatively. The anomalous linear thermal expansion is caused by the predominance of the transversal acoustical phonons over the longitudinal and transversal optical phonons at low temperatures. The third and the fourth terms in formula (20) must be interpreted as correction terms because the temperatures Θ_3 and Θ_4 correspond to frequencies 18.6 and 77.5 THz which lying outside of the range of phonon frequencies in c-Si [10, 15].

3 Dependencies on the statistical factors

In Section 2 it was shown how the total transition strength $N(T)$ varies with temperature. In this section it will be shown how is the total transition strength redistributed among the transition strengths $N_t(T)$ of the individual elementary excitations. The individual elementary excitations can be described in the frame of the quasiparticle approximation as the systems containing variable number of quasiparticles. The two types of quasiparticles important for the interaction of light with matter are the phonons and excitons (*ie* electrons and holes). The transition strengths of the individual elementary excitations can be expressed as

$$N_t(T) = N_t^{300\mathrm{K}}\, f_t(T)\, \mathcal{E}(T)\,, \tag{22}$$

where $N_t^{300\mathrm{K}}$ are the transition strengths of individual contributions at 300 K and $\mathcal{E}(T)$ describes the temperature dependence due to the changes in the density of charged particles. The *statistical factors* $f_t(T)$ express the dependence due to the changes in the mean occupation numbers of the participating quasiparticles, which are governed by the Bose–Einstein and Fermi–Dirac statistics.

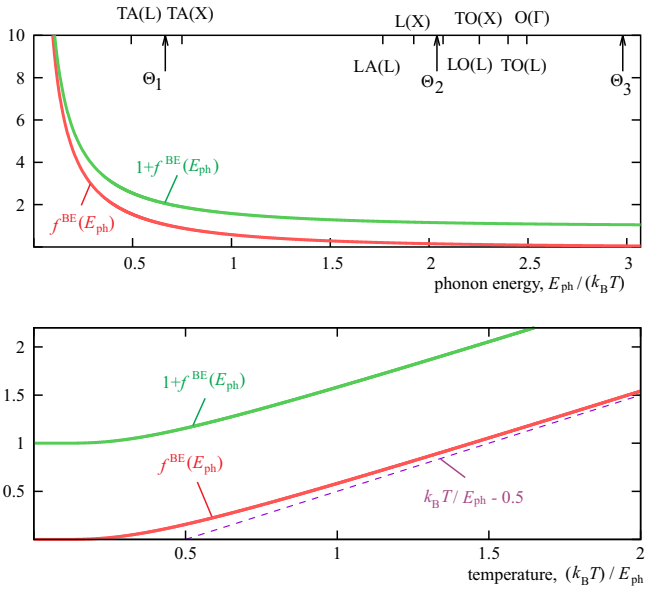

Fig. 3. Bose–Einstein statistical factor $f^{\mathrm{BE}}(E_{\mathrm{ph}}, T)$ as a function of phonon energy or temperature

3.1 Phonons

Phonons are bosonic quasiparticles governed by the *Bose–Einstein statistics*

$$\langle n_{\mathrm{ph}} \rangle = f^{\mathrm{BE}}(E_{\mathrm{ph}}, T) = \frac{1}{\exp\left(\frac{E_{\mathrm{ph}}}{k_{\mathrm{B}}T}\right) - 1}\,, \tag{23}$$

where $\langle n_{\mathrm{ph}} \rangle$ is the mean number of the specific phonons and E_{ph} is the corresponding energy quantum needed for changing the vibrational state of the system (phonon energy). The dependencies of the Bose–Einstein statistical factor $f^{\mathrm{BE}}(E_{\mathrm{ph}}, T)$ on the phonon energy and temperature are depicted in Fig. 3. The positions of the phonon energies of c-Si are calculated at 300 K. The indicated temperatures Θ_1, Θ_2 and Θ_3 of average phonons correspond to the 3rd fit in Tab. 1. The upper panel show the dependence on the phonon energy at constant temperature, whereas the bottom panel shows the dependence on the temperature for the specific phonon energy. The top axis of the upper panel shows the phonon energies of c-Si calculated at 300 K for the directions of the highest symmetries Γ, X and L. From the displayed hierarchy of phonon energies it is obvious that the mean numbers of transversal acoustical phonons (with the lowest energies) are larger than the mean numbers of longitudinal phonons and transversal optical phonons.

The bottom panel of Fig. 3 shows that the mean number of specific phonons is almost zero up to approximately $0.25E_{\mathrm{ph}}/k_{\mathrm{B}}$ and that for high temperatures it behaves as (see the dashed line)

$$\langle n_{\mathrm{ph}} \rangle \approx \frac{k_{\mathrm{B}}T}{E_{\mathrm{ph}}} - \frac{1}{2}\,. \tag{24}$$

The mean number of the phonons with energy E_{ph} at temperature T given by the Bose–Einstein statistics still

fluctuates due to the relaxation (scattering) processes and due to the interaction with the surrounding, *eg* by the absorption or emission of the photons.

The phonons can interact with light by processes in which the phonons are created or annihilated. However, the probabilities of the creation and annihilation processes are not the same. The probability of the phonon annihilation processes is proportional to the number of the excited phonons n_{ph} before the interaction with light whereas the probability of the inverse processes of phonon creation is proportional to the number of the excited phonons after the interaction with light $1 + n_{\mathrm{ph}}$, where n_{ph} is the the number of the excited phonons before the interaction. This is the reason why we decided to plot two curves in Fig. 3. The green curves correspond to the probability of the phonon creation while the red curve corresponds to the probability of annihilation.

Note that, the probability of the creation of the phonon is always higher than the probability of the annihilation of the same phonon even if the system is in the non-equilibrium state. Therefore, the net contribution to the transition strength of the system is positive. This contrasts with electrons, which may give negative contribution in the non-equilibrium states (see Section 3.2).

3.1.1 One-phonon absorption

The dielectric response of the matter must take into account both the photon absorption and the stimulated emission processes. The photon absorption processes contribute positively to the transition strength function while the stimulated emission processes contribute negatively. In the frame of one-phonon processes the interaction of the light is represented by the creation or annihilation of photon with the simultaneous annihilation or creation of phonon with the energy $E = E_{\mathrm{ph}}$. Because the total momentum must be conserved and the momentum of the photon is negligible compared to the momentum of massive (quasi)particle, only the phonons with near-zero momentum $\boldsymbol{k} \approx 0$ can participate in the one-phonon absorption processes. In other words, only the transversal optical (TO) phonons at Γ point in crystalline materials or localized vibrational states existing in both crystalline and disordered materials can interact with the electromagnetic field. Thus, the transition strength function representing one-phonon processes for the specific phonon can be expressed by the delta function weighted by the probability of the individual photon absorption or stimulated emission processes:

$$\begin{aligned} F_{1\mathrm{ph}}(E,T) = N_{\mathrm{ph}}^{300\mathrm{K}} \Big[\big(1 + f^{\mathrm{BE}}(E_{\mathrm{ph}},T)\big)\, \delta(|E| - E_{\mathrm{ph}}) \\ - f^{\mathrm{BE}}(E_{\mathrm{ph}},T)\, \delta(|E| - E_{\mathrm{ph}}) \Big]\, \mathcal{E}(T) = \\ N_{\mathrm{ph}}^{300\mathrm{K}}\, \delta(|E| - E_{\mathrm{ph}})\, \mathcal{E}(T)\,. \end{aligned} \tag{25}$$

It is evident that the Bose–Einstein statistics does not introduce temperature dependence into this final formula. This means that the statistical factor $f_{1\mathrm{ph}}(T)$ of the one-phonon processes in (22) is a constant equal to one. In practice the one-phonon absorption is not described by sharp absorption lines represented by the delta function but by broadened absorption peaks. The Lorentzian broadening function is suitable for the TO phonons in crystalline materials, the Gaussian broadening function is appropriate for the modeling of localized vibrational modes in crystalline or amorphous materials. A more general model of the broadening function is the Voigt function representing the convolution of the Lorentzian and the Gaussian functions. The most general models use the asymmetric Voigt profiles. The phonon absorption peaks with asymmetric shapes represent couplings between the vibrational modes or the Fano resonance (quantum interference between electrons and phonons).

Although there are TO phonons at the Γ point in the c-Si crystal, they do not contribute to the one-phonon absorption. The reason is that the crystalline silicon is a homopolar material with purely covalent bonds and for such materials the probability of the excitation of the TO phonon by the interaction with light is zero. The homopolar materials exhibit one-phonon absorption only on the localized vibrational states, *ie* if the crystal structure contains defects. In the c-Si such defect can be, for example, the interstitial oxygen. The interstitial oxygen with the typical concentration 20 ppm occurs in the Czochralski silicon used commonly in the electronics industry. The strength of the absorption structures caused by the interstitial oxygen is linearly proportional to the concentration of the interstitial oxygen but it is independent on the temperature. The interstitial oxygen causes presence of several localized vibrational modes of the O atoms which can be modeled using the Gaussian broadened discrete spectrum and vibrational modes of the Si atoms forming the absorption band. The absorption band corresponds to the vibration of the Si atoms in the vicinity of the O atoms where the translation symmetry is broken. These modes correspond to the vibration of the Si–Si bonds and their energies cover the whole range from zero to the maximal phonon energy in c-Si at the Γ point. This absorption band can be modeled by the Gaussian broadened piecewise polynomial function. For details see our previous work [9].

3.1.2 Multi-phonon absorption

The multi-phonon absorption is a weak effect in general, therefore, it is observable only as the attenuation of light in relatively thick partially transparent slabs. It can be neglected in the dispersion models for thin films. As the number of the participating phonons increases the strength of the multi-phonon absorption decreases and the absorption structures extend to higher frequencies. The multi-phonon absorption is usually visible only in the spectral regions where it is not masked by other absorption structures. For example, the complete two-phonon absorption structure can be observed only in materials

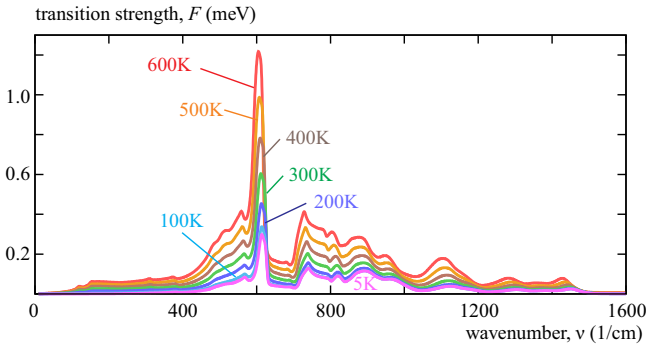

Fig. 4. Spectral dependencies of the transition strength function of the float zone c-Si corresponding to the phonon absorption contributions at various temperatures

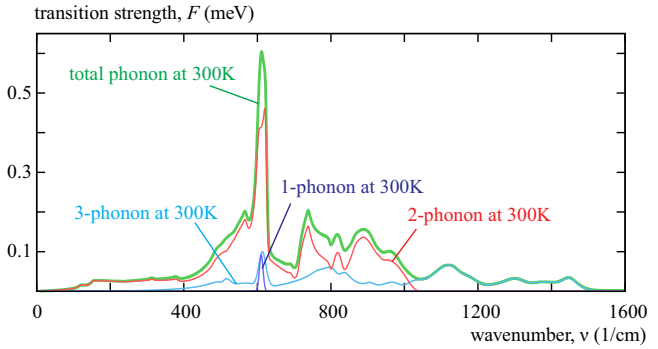

Fig. 5. Separation of the transition strength function of the float zone c-Si into contributions representing the one-, two- and three-phonon absorption

where the one-phonon absorption is weak, *ie* in the homopolar materials, otherwise, the lower half of the spectral range in which this absorption occurs is masked by much stronger one-phonon absorption.

The statistical factors in (22) for the two-phonon absorption can be derived by the same procedure as in the last section. If the two participating phonons are denoted A and B, then the following well known [22, 23] temperature dependent statistical factors can be derived:

$$f_{2\mathrm{ph(A+B)}}(T) = 1 + f^{\mathrm{BE}}(E_{\mathrm{A}}, T) + f^{\mathrm{BE}}(E_{\mathrm{B}}, T) \qquad (26)$$

and

$$f_{2\mathrm{ph(A\text{-}B)}}(T) = f^{\mathrm{BE}}(E_{\mathrm{A}}, T) - f^{\mathrm{BE}}(E_{\mathrm{B}}, T)\,. \qquad (27)$$

The first statistical factor corresponds to the absorption processes where both the phonons are created or annihilated, whereas the second statistical factor corresponds to the absorption processes where one phonon is created and the other is annihilated. The statistical factors governing the two-phonon absorption processes depend linearly on the Bose–Einstein statistical factors of individual phonons. These statistical factors can be easily used for expressing the transition strength of the two-phonon absorption on localized vibrational modes. The above results were derived for two phonons with specific energies. The complete description of the two-phonon absorption in crystalline materials is relatively complicated task leading to absorption bands which combine contributions from all pairs of phonons with zero total momentum. Nevertheless, the transition strength in the resulting model still exhibits the linear dependence on the Bose–Einstein statistical factors. The details concerning this model applied to c-Si are described in our previous works [7, 10].

The three- and four-phonon absorption processes are also included in our temperature dependent dispersion model of c-Si. These absorption bands are modeled by the Gaussian broadened piecewise polynomial function with statistical factors assuming only simultaneous creation or simultaneous annihilation of three or four phonons, *ie*

$$f_{3\mathrm{ph}}(T) = 1 + 3f^{\mathrm{BE}}(E_{3\mathrm{ph}}/3, T) + 3[f^{\mathrm{BE}}(E_{3\mathrm{ph}}/3, T)]^2 \qquad (28)$$

and

$$f_{4\mathrm{ph}}(T) = 1 + 4f^{\mathrm{BE}}(E_{4\mathrm{ph}}/4, T) + 6[f^{\mathrm{BE}}(E_{4\mathrm{ph}}/4, T)]^2 + 4[f^{\mathrm{BE}}(E_{4\mathrm{ph}}/4, T)]^3\,. \qquad (29)$$

It should be noted that these formulas were derived with the assumption that all the participating phonons have the same energy.

The spectral dependencies of the transition strength function corresponding to the phonon absorption of the float zone c-Si calculated by our model for temperatures in the range from 5 to 600 K are plotted in Fig. 4. Since the one-, two-, three- and four-phonon absorption structures exhibit different dependencies on temperature, it is possible to distinguish these processes if the temperature dependent data are available [11]. The separation of the transition strength function calculated at 300 K into parts corresponding to the one-, two- and three-phonon processes is shown in Fig. 5 (the four-phonon absorption structures are too weak to be displayed in this figure). The float zone c-Si is the purest commonly available crystalline silicon free of the interstitial oxygen. The one-phonon processes correspond to the localized vibrational modes of the substitutional carbon in the Si lattice.

3.2 Excitons

Excitons are fermionic quasiparticles governed by the *Fermi–Dirac statistics*

$$\langle n_{\mathrm{e}} \rangle = f^{\mathrm{FD}}(E_{\mathrm{e}}, T) = \frac{1}{\exp\left(\frac{E_{\mathrm{e}} - \mu}{k_{\mathrm{B}} T}\right) + 1}\,, \qquad (30)$$

where $\langle n_{\mathrm{e}} \rangle$ is the mean number of electrons in the given single-particle state with the energy E_{e} and μ is the *chemical potential*. In general, the chemical potential changes with the temperature T but in many cases it can be assumed to be constant with the value given by the *Fermi energy* $\mu(T) \approx \mu(0) = E_{\mathrm{F}}$. Moreover, Fermi energy can be set in arbitrary value, usually $E_{\mathrm{F}} = 0$. The Fermi energy lies between the energies of the highest occupied and the lowest unoccupied single-particle states

in the ground state of the system, *ie* at $T = 0$. The number of electrons in the given state n_e can be either 0 or 1, thus, the mean number of electrons is between 0 an 1 (see the red curves in Fig. 6). The temperature dependencies are plotted for electrons $f^\mathrm{FD}(E_\mathrm{e}, T)$ and holes $1 - f^\mathrm{FD}(E_\mathrm{e}, T)$ in the conduction band (above the Fermi energy). In the valence band ($E_\mathrm{e} - \mu < 0$) the curves exhibit the opposite trend. If the single-electron state is unoccupied $n = 0$, it is possible to say that in this state is a hole. A complementary statistical factor $1 - f^\mathrm{BE}(E_\mathrm{e}, T)$ expressing the probability that the single-electron state is unoccupied can be defined for holes (see the green curves in Fig. 6). Although, the number of electrons in the given state fluctuates, the total number of the electrons in the system is constant, *ie* each empty state below the Fermi energy must be accompanied by a filled state above the Fermi energy. The pairs of the unoccupied (holes) and occupied (electrons) states are called excitons.

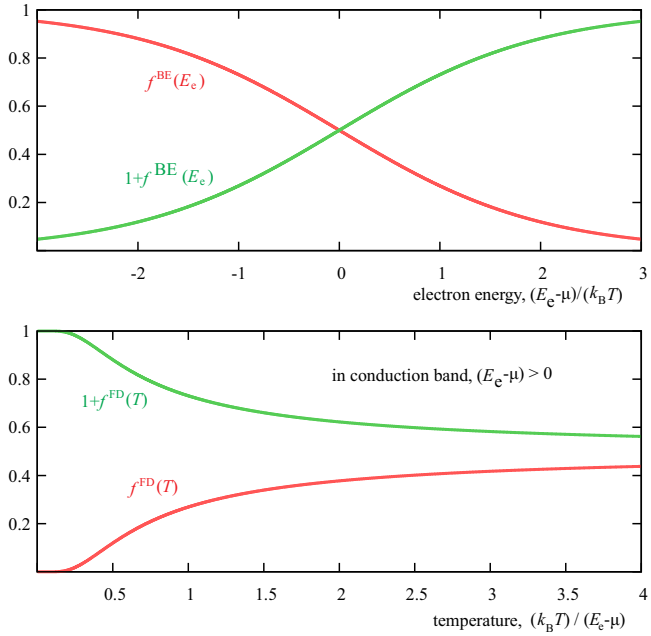

Fig. 6. Fermi–Dirac statistical factor $f^\mathrm{FD}(E_\mathrm{e}, T)$ as a function of electron energy or temperature

The transitions of the electron between two specified single-electron states differing by the energy E can be stimulated by light. The transition of the system from the lower to the higher energy state corresponds to the photon absorption process, whereas the reverse transition corresponds to the stimulated emission process. The probabilities of both the processes are the same and, therefore, the transition strength of the excitation process is given by the occupation numbers of electrons and holes in the initial and final states as follows

$$\begin{aligned} F_\mathrm{ex}(E,T) \propto \mathcal{E}(T)\Big[& \\ & f^\mathrm{FD}(E_\mathrm{e},T)\big(1 - f^\mathrm{FD}(E_\mathrm{e}+E,T)\big)\,\delta(|E| - E_\mathrm{ex}) \\ & - f^\mathrm{FD}(E_\mathrm{e}+E,T)\big(1 - f^\mathrm{FD}(E_\mathrm{e},T)\big)\,\delta(|E| - E_\mathrm{ex}) \\ & \Big] \approx \mathcal{E}(T)\,\delta(|E| - E_\mathrm{ex}). \end{aligned} \tag{31}$$

The first positive term in the square brackets corresponds to the absorption process and the second negative term corresponds to the stimulated emission process. In the thermodynamic equilibrium the size of the first positive term is always larger than the size of the second negative term, thus, the net strength is positive. This is not true for non-equilibrium states of the system where the transition strength function can be negative in some spectral region. This is because the certain part of the system exhibits the inverse population of electrons, which corresponds to the negative T. Of course, the sum rules must be fulfilled even for the non-equilibrium states, therefore, the total transition strength must be positive. In dielectrics the initial and final states of the interband transitions are sufficiently far from the Fermi energy (the temperature 300 K corresponds to the energy 0.026 eV). This means that the statistical factors of the first terms are close to unity and the statistical factors of the second terms are close to zero. Therefore, the interband transitions in dielectrics are independent on the Fermi–Dirac statistical factors. Of course, this statement is not valid for the interband transitions in metals or indirect intraband transitions in the infrared region.

3.2.1 Free-carrier contribution

The density of the holes $\mathcal{N}_\mathrm{h}$ below and the density of the electrons $\mathcal{N}_\mathrm{e}$ above the Fermi energy depend strongly on the Fermi–Dirac statistical factor:

$$\mathcal{N}_\mathrm{h}(T) = \int_{-\infty}^{E_\mathrm{F}} \big(1 - f^\mathrm{FD}(E_\mathrm{e}, T)\big)\ \mathcal{D}_\mathrm{e}(E_\mathrm{e})\ \mathrm{d}E_\mathrm{e} \tag{32}$$

and

$$\mathcal{N}_\mathrm{e}(T) = \int_{E_\mathrm{F}}^{\infty} f^\mathrm{FD}(E_\mathrm{e}, T)\ \mathcal{D}_\mathrm{e}(E_\mathrm{e})\ \mathrm{d}E_\mathrm{e}\,, \tag{33}$$

where $\mathcal{D}_\mathrm{e}(E_\mathrm{e})$ is the electron *density of states* (DOS) function. Since it must hold $\mathcal{N}_\mathrm{h}(T) = \mathcal{N}_\mathrm{e}(T)$, it is evident that if the DOS function is asymmetrical owing to the Fermi energy, then it is necessary to consider temperature dependent chemical potential. Moreover, the DOS functions are also slightly temperature dependent. Although finding the temperature dependent model of the density of free carriers can be relatively complicated task in general, for specific materials it is possible to use a relatively simple formulas based on certain simplifying assumptions.

In the case of c-Si it possible to use the following assumptions. The shape of the electron dispersion function $E_\mathrm{e}(\boldsymbol{k})$ in the vicinity of the maximum of the valence band is quadratic. The same is true for the minimum of the conduction band. The DOS function of electrons can be then approximated by two square root functions positioned symmetrically around the Fermi energy, which lies in the middle between the bands (see Fig. 7).

The density functions are shown in arbitrary units. The functions $\mathcal{N}_\mathrm{e}(E_\mathrm{e})$ and $\mathcal{N}_\mathrm{h}(E_\mathrm{e})$ are scaled by factors

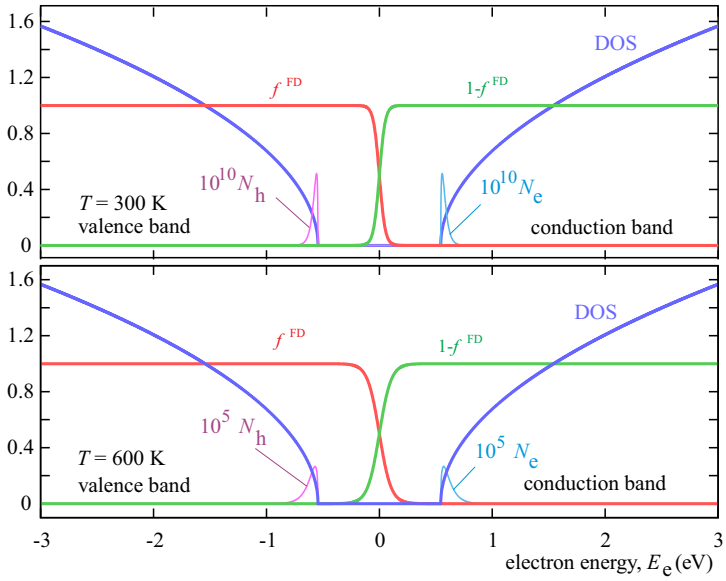

Fig. 7. Distribution of the electrons $\mathcal{N}_e(E_e)$ and holes $\mathcal{N}_h(E_e)$ in the conduction and valence bands calculated for temperatures 300 K and 600 K

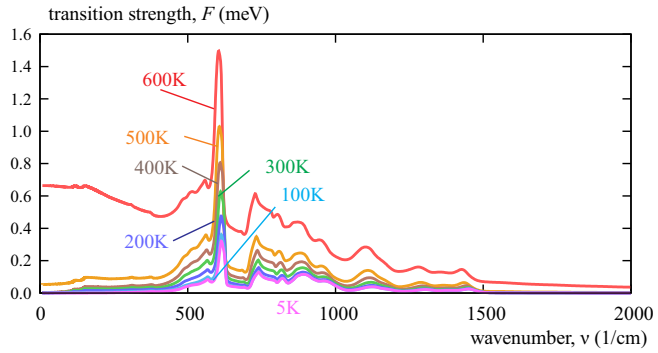

Fig. 8. Spectral dependencies of the transition strength function of the float zone c-Si at various temperatures including both the free-carrier and phonon contributions

introduced in the legend. The Fermi energy is assumed to be in the middle of the bands and it corresponds to the zero level, *ie* $E_F = 0$. The red and green curves represent the Fermi-Dirac statistics of electrons and holes, respectively. Moreover, it will be assumed that the DOS function depends linearly only on the expansion factor $\mathcal{E}(T)$ and the processes involve only the creation or annihilation of one phonon. The density of free carriers in the valence and conduction bands is then proportional to the following integral

$$\mathcal{N}_{fc}(T) \propto \mathcal{E}(T) \int_{E_g/2}^{\infty} f^{FD}(E_e, T)\, \sqrt{E_e - E_g/2}\, dE_e$$
$$\propto \mathcal{E}(T) \sum_{i=1}^{\infty} (-1)^{i-1} \left(\frac{T}{i}\right)^{3/2} \exp\left(-\frac{iE_g}{2k_B T}\right), \quad (34)$$

where $E_g/2$ is the distance of the bands from the Fermi level. The free-carrier contribution corresponds to the processes involving creation or annihilation of phonons (indirect intraband transitions), thus, the transition strength is proportional to the density of free carriers multiplied by the Bose-Einstein statistical factor representing the probability of the creation and annihilation of one average phonon:

$$N_{fc}(T) \propto \mathcal{N}_{fc}(T)\left(1 + 2f^{BE}(E_{ph}, T)\right). \quad (35)$$

For sufficiently small energies only the first term in expression for the integral (34) can be taken into account. This is equivalent to neglecting the unity in the denominator of the Fermi–Dirac statistical factor, which corresponds to replacing the quantum-mechanical Fermi–Dirac statistic by the classical Maxwell–Boltzmann statistic. Moreover, the Bose–Einstein statistical factor in (35) can be omitted at low temperatures. Under these assumptions the transition strength of free carriers in c-Si can be modeled by the well known formula [24]

$$N_{fc}(T) \propto T^{3/2} \exp\left(-\frac{E_g}{2k_B T}\right) \mathcal{E}(T). \quad (36)$$

If this factor is rewritten with respect to the reference temperature used in our dispersion model of c-Si, then we arrive to the following simple form for the statistical factor used in (22) for free carriers:

$$f_{fc}(T) = \left(\frac{T}{T_R}\right)^{3/2} \exp\left(-\frac{E_g(T_R - T)}{2k_B T T_R}\right). \quad (37)$$

The model used for the normalized transition strength function $F^0_{fc}(E)$ is based on the modification of the Drude formula [7, 11]. The influence of the free-carrier contribution on the transition strength function in the region of phonon absorption is visible in Fig. 8 for curves calculated at temperatures 500 and 600 K (compare with Fig. 4). Since the energies of the optical phonons are comparable

with the energies corresponding to these temperatures, the revised version of c-Si includes the influence of the Bose–Einstein statistical factor present in formula (35). However, it should be noted that this change had only very small influence on the accuracy of the dispersion model.

3.2.2 Indirect interband transitions in crystals

In the case of dielectrics the influence of the Fermi–Dirac statistical factors can be neglected, therefore, the temperature dependence of the transition strength will be determined only by the Bose–Einstein statistical factors corresponding to creation and annihilation of phonons. Since the energy of the phonon E_{ph} contributes differently to the energy conservation law when the phonon is created and annihilated, it is necessary to consider two branches of the contributions differing only in the sign of the phonon energy. The transition strength function for both the branches can be expressed as:

$$\begin{aligned} F_{\mathrm{IDT}}(E,T) = \frac{N_{\mathrm{IDT}}^{300\mathrm{K}}\,\mathcal{E}(T)}{1+2f^{BE}(E_{\mathrm{ph}},T_{\mathrm{R}})}\Big[\\ f^{BE}(E_{\mathrm{ph}},T)\; F^{0}_{\mathrm{IDT}}(E-E_{\mathrm{ph}},T) + \\ \big(1+f^{BE}(E_{\mathrm{ph}},T)\big)\; F^{0}_{\mathrm{IDT}}(E+E_{\mathrm{ph}},T)\;\Big], \end{aligned} \tag{38}$$

where the first term corresponds to the process in which the phonon is annihilated and the second term corresponds to the process in which the phonon is created. The normalized transition strength functions $F^{0}_{\mathrm{IDT}}(E \pm E_{\mathrm{ph}},T)$ are identical for both the terms, the only difference is in the sign of the E_{ph} in their arguments. This means that the two branches are mutually shifted by the energy $2E_{\mathrm{ph}}$. However, the strength of each of the branches is governed by a different statistical factor. The strength of the phonon creation branch (the second term) is always higher than the strength of the phonon annihilation branch (the first term), which completely disappears at zero temperature.

The phonon energy E_{ph} plays two roles in formula (38). Firstly, it determines the temperature dependence of the statistical factor. Secondly, it determines the shift of the creation and the annihilation branches, which is especially important for materials with the indirect band gap. In these materials the absorption edge in the vicinity of the band gap energy E_{g} has a complex shape and it corresponds to a series of overlapping absorption edges. In c-Si a relatively good model can be obtained using only one phonon energy [23, 25], but a model using several phonon energies provides more accurate description [11]. It is well known [23] that the indirect absorption edge in c-Si is realized by electronic transitions from the Γ point to the point near the X direction. Since the momentum in the Γ point is zero, the momentum of the participating phonons must correspond to the momentum near the X point. In the work [11] three phonon energies corresponding to frequencies $f_{\mathrm{TO(X)}}$, $f_{\mathrm{L(X)}}$ and $f_{\mathrm{TA(X)}}$ were considered. In the current version of c-Si it is assumed that the momentum of the phonons does not correspond to the X point but to a point slightly shifted towards the Γ point. Since the degeneracy of the longitudinal phonons disappears, four phonon energies corresponding to TO, LO, LA and TA branches are used.

3.2.3 Transitions involving localized states

There are various origins of the existence of localized states in the condensed matter. The first class of localized states is connected with the existence of defects such as vacancies, impurities, dangling bonds *etc.* The transition strengths of these localized states are proportional to the densities of defects and, therefore, their temperature dependencies are weak. In our models their temperature dependencies are only through the expansion factor $\mathcal{E}(T)$. The second group of localized states is connected with the disorder of atoms. The disorder of atoms increases with the temperature due to the increase in the phonon occupation numbers. These localized states also exist in the ideal crystals without any defect at zero temperature, because the nuclei fluctuate around the equilibrium positions even in the ground state. Thus, the transition strengths of the processes involving localized states are described by the statistical factors which contain the constant parts and also the temperature dependent parts. The constant parts describe the first class of the localized states and the contribution corresponding to the ground state of the second class. The temperature dependent parts, which are given by the ABESF, describe the effect of the increasing disorder due to the thermal motion of the nuclei. The statistical factor in (2) can be written as

$$f_{\mathrm{ut}}(T) = \frac{1}{1+C}\left[1 + C\frac{\exp(\Theta/T_{\mathrm{R}})-1}{\exp(\Theta/T)-1}\right], \tag{39}$$

where the constant C and the average phonon temperature Θ describe the temperature dependent part.

In the c-Si the localized states represent a weak effect which is observable only if special spectroscopic methods are used (*eg* the deflection spectroscopy). In the current model of c-Si the localized states are represented by the weak Urbach tail corresponding to weak absorption below the band gap. The Urbach tail was included into the model on the basis of the transmittance measurements of 14 mm thick slab at the room temperature. Since only the room temperature data were used, the transition strength of the Urbach tail is given by the constant statistical factor without the ABESF term, *ie* $C = 0$ in (39).

3.2.4 High energy electron excitations

The strengths of the excitations of the valence electrons to the empty high energy electron states or the excitations of the core electrons are not influenced by the temperature dependent statistical factors. Therefore, the temperature dependence of the transition strengths of these excitations is only through the expansion factor. The high energy valence electron excitations can be modeled by dispersion models based on the combination of the Tauc's law with the Lorentz model [26], which are usually used for interband transitions. For example, the Campi–Coriasso [27] dispersion model is appropriate if accurate description in the X-ray region is not required. The Lorentz model has the classical asymptotic behavior for high energies which does not accurately describe scattering processes in the X-ray region (see discussion in [7]).

This part of the c-Si dispersion model is still under development. The current version uses only simple models with the classical asymptotic behavior describing both the high energy valence electron excitations and the core electrons excitations. The current model is correct in the region of low energies and has no ambitions to describe the dielectric response perfectly in the X-ray region (see [11]).

3.2.5 Direct interband transitions in crystals

It is not easy to describe the temperature dependence of the direct interband transitions in crystals because the temperature dependence due to the Fermi–Dirac statistical factor is weak in comparison with the temperature dependencies of the matrix elements. The temperature dependencies of the matrix elements, especially the temperature dependencies of the excitonic many body effects, cause relatively strong redistribution of the transition strength function but the integral value of the transition strength is nearly temperature independent. The sum rule can be used to express the temperature dependence of the transition strength. The following formula can be derived on the basis of (14), (17) and (22)

$$N_{\mathrm{DT}}(T) = \Big[N^{300\mathrm{K}} - \sum_{t}^{t\neq\mathrm{DT}} N_t^{300\mathrm{K}}\, f_t(T)\Big]\, \mathcal{E}(T)\,. \qquad (40)$$

The first term in the square brackets represents the total transition strength and the sum represents the total transition strength of all the contributions other than the direct transitions (DT). Thus, the weak temperature dependence of the transition strength of the direct transitions is given by the expansion factor $\mathcal{E}(T)$ and the temperature dependencies of the other contributions. The formula (40) represents the basic idea behind the temperature dependent dispersion models in crystalline solids.

3.2.6 Interband transitions in disordered materials

In disordered materials the direct transitions (transitions not involving phonons) are indistinguishable from indirect transitions (those involving phonons), therefore, they are treated as one contribution to the dielectric response. The basically same idea that was used to calculate the strength of the direct transitions in crystalline materials can be used for disordered condensed materials, *ie* amorphous solids and liquids. The temperature dependent transition strength of the interband transitions (IBT) is described by the equation equivalent to (40) as

$$N_{\mathrm{IBT}}(T) = \Big[N^{300\mathrm{K}} - \sum_{t}^{t\neq\mathrm{IBT}} N_t^{300\mathrm{K}}\, f_t(T)\Big]\, \mathcal{E}(T)\,. \qquad (41)$$

The normalized transition strength function of the disordered materials can be described using the models unifying all the valence electron excitations, *ie* interband transitions and the high energy excitations of valence electrons. The examples of such models are the Campi–Coriasso [27], Jellison–Modine [28, 29] (known as the Tauc–Lorentz) or Ferlauto *et al* [30] (known as the Cody–Lorentz) models, which combine the Tauc's law and the Lorentz model [26]. We should note that for the purposes of our temperature dependent dispersion model it is necessary to perform the proper sum rule normalization of these models.

Nevertheless, it should be noted that in principle it is possible to separate the interband transitions into the valence to conduction band transitions and into the high energy excitations of valence electrons since each of them has different dependence on temperature. This separation is convenient if the experimental data extending to the synchrotron spectral region are processed [31-33].

4 Red shift of characteristic energies

The characteristic energies (critical point energies of direct electron excitations, indirect band gap energies, phonon energies, *etc*) usually decrease with the increasing temperature, thus we are saying that they exhibit red shift [34-38]. However, the opposite trend (blue shift) is sometimes observed, for example, the shift of the band gap energy of PbTe [39] or the shift of the phonon frequency in the body-centered cubic molybdenum [40]. The shifts of characteristic energies of electrons and phonons are due to the thermal expansion (growing distances between the atoms) and as a consequence of the electron-phonon [34] and phonon-phonon [40] interaction. These effects depend approximately linearly on the phonon occupation numbers, therefore, the formulas based on the ABESF can be used to model the temperature dependencies of the characteristic energies.

In our c-Si model the temperature dependencies of the band gap energy E_{g} and the critical point energies E_1,

Table 2. Values of the dispersion parameters used to calculate the band gap and critical point energies

	standard notation	E_j^{0K} (eV)	E_j^{300K} (eV)	Θ_j (K)	model Eq.
$E_3'(\mathrm{X})$		–	18.37	–	(45)
$E_3(\mathrm{X})$		–	14.43	–	(45)
$E_2''(\mathrm{X})$		–	14.01	–	(45)
$E_2'(\mathrm{X})$		–	10.07	–	(45)
$E_1(\Gamma)$		–	8.501	–	(45)
$E_0(\Sigma)$		–	7.657	–	(45)
$E_3(\Sigma)$		–	7.066	–	(45)
$E_3(\Delta)$		6.759	6.766	1016.0	(42)
$E_1'(\mathrm{L})$	E_1'	5.347	5.307	739.1	(42)
$E_2(\Sigma)$		4.456	4.384	–	(43)
$E_2(\mathrm{X})$	E_2	4.331	4.298	674.8	(42)
$E_1(\mathrm{K})$		4.238	4.204	–	(43)
$E_0(\Gamma)$	E_0	–	4.023	–	(45)
$E_1(\mathrm{L})$	E_1	3.421	3.391	538.8	(42)
$E_0'(\Gamma)$	E_0'	3.399	3.369	–	(43)
E_g		1.134	1.086	382.9	(42)

$E_2(\mathrm{X})$, E_1' and $E_3(\Delta)$ are described using a simple three-parametric model

$$E_j(T) = E_j^{0\mathrm{K}} + \left(E_j^{300\mathrm{K}} - E_j^{0\mathrm{K}}\right)\frac{\exp(\Theta_j/T_\mathrm{R}) - 1}{\exp(\Theta_j/T) - 1}, \quad (42)$$

where Θ_j is the average photon energy (temperature), $E_j^{0\mathrm{K}}$ and $E_j^{300\mathrm{K}}$ are the band gap or critical point energies corresponding to the zero absolute temperature and the reference temperature 300 K. Owing to the accuracy of the optical measurements, it is sufficient to use the formulas using only one ABESF term. The temperature dependencies of the band gap and critical points energies used in our c-Si model are depicted in Fig. 9. The dependencies calculated using the formula (42) are plotted in red color and the corresponding values of the parameters are introduced in Tab. 2. The horizontal lines separate the critical points into groups in which the energies $E_j(T)$ in formulas (45) and (43) are calculated using the three-parametric model (42) belonging to the same group.

In some cases the critical point energies lie very close to each other (*eg* for the M_0 type critical point E_0' and M_1 type critical point $E_1(\mathrm{L})$ in c-Si) and their distance decreases with the increasing temperature. In this case it is necessary to ensure that the hierarchy of the critical points energies is the same at all temperatures ($E_1(L) > E_0'$). The temperature dependencies of such two critical point energies $E_j(T)$ and $E_j'(T)$ can be then described by a five-parametric model.

The temperature dependence of the energy $E_j(T)$ is modeled by formula (42) and the temperature dependence of the energy $E_j'(T)$ is given by the following formula

$$E_j'(T) = E_j(T) + (E_j'^{0\mathrm{K}} - E_j^{0\mathrm{K}})\exp\left(-\mathcal{L}\frac{T}{T_\mathrm{R}}\right), \quad (43)$$

where $E_j'^{0\mathrm{K}}$ and $E_j'^{300\mathrm{K}}$ are the energies at 0 K and 300 K. The positive constant $\mathcal{L}$ is calculated as

$$\mathcal{L} = \ln\left(\frac{E_j'^{0\mathrm{K}} - E_j^{0\mathrm{K}}}{E_j'^{300\mathrm{K}} - E_j^{300\mathrm{K}}}\right). \quad (44)$$

In our c-Si model this formula is used for the critical points energies E_0', $E_1(\mathrm{K})$ and $E_2(\Sigma)$ (see Fig. 9 and Tab. 2), The experimental points are taken from Frey *et al* work [41]. From the Fig. 9 it can be seen that the dependencies calculated using (43) are almost parallel with those calculated using (42). The critical point E_0 is assumed to have the temperature dependence given by the same ABESF term as E_2, *ie* the curves describing their temperature dependencies are parallel. The remaining critical points lying above $E_3(\Delta)$ are assumed to have

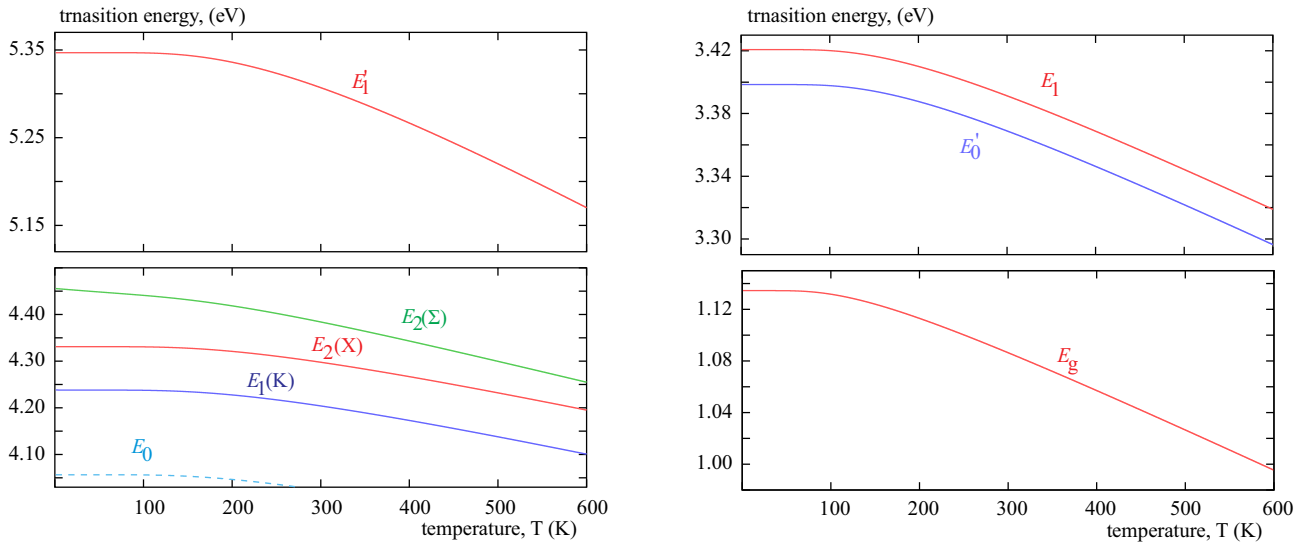

Fig. 9. Temperature dependencies of the band gap and critical point energies used in our dispersion model of c-Si

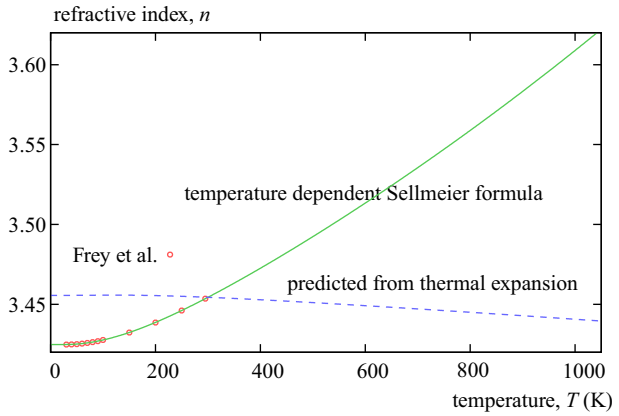

Fig. 10. Temperature dependence of the refractive index of c-Si at wavelength $\lambda = 2\,\mu\mathrm{m}$

the temperature dependencies given by the same ABESF term as $E_3(\Delta)$. Thus, it is possible to define these critical points by introducing only one additional parameter specifying the value at 300 K (see Tab. 2). The critical point energies $E'_j(T)$ are then calculated as

$$E'_j(T) = E_j(T) + {E'}_j^{300\mathrm{K}} - E_j^{300\mathrm{K}}\,, \tag{45}$$

where $E_j(T)$ is calculated using the formula (42).

Table 3. Values of the dispersion parameters of the temperature dependent two-term Sellmeier formula (46) of c-Si determined by fitting the Frey *et al* data [41]

j	N_j (eV^2)	$E_j^{0\mathrm{K}}$ (eV)	$E_j^{300\mathrm{K}}$ (eV)	Θ_j (K)
1	273.563	4.38129	4.36617	592.56
2	23.447	3.24469	3.10798	208.97

The correctness of the formulas with only one ABESF term can be also demonstrated on the temperature dependence of the refractive index of c-Si in the near infrared region where it is transparent. The Frey *et al* measured the refractive index of the float zone c-Si prism using the minimal deviation method with very low uncertainty 1×10^{-4} [41]. Their measurements were performed in the helium cryostat from very low temperatures up to the room temperature (see the experimental data from 30 to 295 K at the wavelength $\lambda = 2\,\mu\mathrm{m}$ in Fig. 10). In our previous paper [11] it was shown that it is possible to fit the Frey's data with very high accuracy by the temperature dependent two-term Sellmeier formula

$$n^2(E,T) - 1 = \frac{2}{\pi}\sum_{j=1}^{2}\frac{N_j}{E_j^2(T) - E^2}\,, \tag{46}$$

where the temperature dependencies of the energies $E_j^2(T)$ are modeled using the three-parametric formula for the critical point energies (42). This model depends on eight parameters introduced in Tab. 3. If it was assumed that the temperature dependence of the refractive index is given only by the expansion factor and the shifts of the energies were disregarded, then the refractive index at the wavelength $2\,\mu\mathrm{m}$ would be calculated as

$$n(2\,\mu\mathrm{m}, T) = n(2\,\mu\mathrm{m}, T_\mathrm{R})\sqrt{\mathcal{E}(T)}\,. \tag{47}$$

The calculated curve in Fig. 10 shows that this dependence does not agree with the experimental data. This is because it is not enough to consider the thermal expansion but the redistribution of the transition strength and the shifts of the characteristic energies must also be considered if we want to obtain the correct dependence on the temperature.

The transitions strengths of the multi-phonon absorption and free-carrier contribution grow with temperature on the expense of the transition strength of the interband transitions of valence electrons. Both the thermal expansion and the redistribution of the transition strength due to the statistical factors predict that the refractive index should decrease with the temperature in the transparent region. The increase in the refractive index can be explained only by the red shift of the characteristic energies, which is, in general, the dominant effect in the transparent region of dielectrics. In fact, the temperature dependence due to the expansion factor is neglected in (46) and the temperature independent parameters N_j are used.

While each critical point energy has its own average phonon temperature determining its temperature dependence, in the case of c-Si it is enough to consider only one average phonon temperature to model the shifts of phonon frequencies. Moreover, it is assumed that the ratio f_ν of phonon frequency at 0 K and frequency at 300 K is the same for all the phonons. The following formula is then used for frequencies $\nu_\mathrm{ph}(T)$ of individual phonons

$$\nu_\mathrm{ph}(T) = \nu_\mathrm{ph}^{300\mathrm{K}}\left[f_\nu + (1-f_\nu)\frac{\exp(\Theta/T_\mathrm{R})-1}{\exp(\Theta/T)-1}\right], \tag{48}$$

where $\nu_\mathrm{ph}^{300\mathrm{K}}$ is the phonon frequency at 300 K.

5 Temperature dependencies of the broadening parameters

The two effects causing the broadening of the dielectric functions are the finite life-time of the single-particle states and the disorder in the materials. Since phonons play a major role in the decay of the single-particle states, the temperature dependence of this part, which corresponds to the Lorentzian broadening in the case of phonons and the Gaussian broadening for electronic excitations, is given by the changes in the phonon occupation numbers. Therefore, the ABESF formula can be used for the broadening parameters

$$B(T) = B^{0\mathrm{K}} + \left(B^{300\mathrm{K}} - B^{0\mathrm{K}}\right)\frac{\exp(\Theta/T_\mathrm{R})-1}{\exp(\Theta/T)-1}\,, \tag{49}$$

where B^{0K} and B^{300K} are the values at 0 K and 300 K. The broadening due to the disorder in the material, which usually corresponds to the Gaussian broadening, can be assumed to be independent on temperature.

In our c-Si model the Gaussian broadening with temperature independent broadening factors was found to be sufficient for interpreting the temperature dependent experimental data in the region of the two- and three-phonon absorption. This shows that the disorder due to the random distribution of different isotopes in the crystal lattice is the dominant effect. The direct interband transitions of valence electrons were modeled using the Gaussian broadening with the temperature dependence of the broadening factors given by (49).

6 Temperature dependence of the Urbach energy

The increasing disorder due to the thermal motion of the nuclei affects not only the transition strength of the Urbach tail (see section 3.2.3) but also the Urbach energy. Therefore, the temperature dependence of the Urbach energy can be modeled by means of one ABESF term as follows

$$E_{\mathrm{u}}(T) = E_{\mathrm{u}}^{0\mathrm{K}} + \left(E_{\mathrm{u}}^{300\mathrm{K}} - E_{\mathrm{u}}^{0\mathrm{K}}\right) \frac{\exp(\Theta/T_{\mathrm{R}}) - 1}{\exp(\Theta/T) - 1}\,. \quad (50)$$

7 Temperature dependencies of the matrix elements

The temperature dependence of the direct interband transitions cannot be modeled correctly if the matrix elements are assumed to be temperature independent because the matrix elements are sensitive to the changes in the band structure. The empirical formulas must be used to model the spectral redistribution of the normalized transition strength function of direct transitions. In our c-Si model we use empirical approach based on the cubic splines. In order to ensure that the transition strengths of the individual contributions are always positive, the cubic splines are used to interpolate the logarithms of the weights of the individual contributions (see weights A_i in [7]).

The many body effects also influence the spectral redistribution of the normalized transition strength of direct transitions. The strength of attraction between the electron–hole pairs is in our model [7] characterized by the Rydberg parameters. Since it was not possible to determine their temperature dependencies on the basis of the available experimental data, it was assumed that these parameters are constant in our c-Si model.

8 Conclusion

The main aim of this work was to discuss the ideas for modeling the temperature dependencies of transition strengths corresponding to the elementary phonon and electron excitations. It was shown that the temperature dependence of the total transition strength is given solely by the expansion factor, which expresses the changes in the density of particles. The distribution of the total transition strength among the individual contributions is controlled by the statistical factors, which are derived on the basis of the Bose–Einstein and Fermi–Dirac statistics of the quasiparticles participating in the absorption processes. The models describing the red shift of characteristic energies and the temperature dependencies of the broadening parameters, Urbach energy and matrix elements were also discussed.

While the temperature dependencies of the transition strengths of the individual absorption processes were described in detail, the concrete forms of the corresponding normalized transition strength functions were not discussed. The overview of the models representing the elementary excitations can be found in [7].

The presented ideas are used in our temperature dependent dispersion model of c-Si. This model is accurate enough to replace the tabulated values of the optical constants of silicon wafers used to interpret the temperature dependent experimental data in the optical characterization of thin films.

Acknowledgements

We would like to thank Dr. René Schödel for supplying the raw measured data of the temperature dependence of the length of the silicon sample used in [16]. This research has been supported by the project LO1411 (NPU I) funded by Ministry of Education, Youth and Sports of Czech Republic.

References

[1] F. Wooten, *Optical Properties of Solids*, New York: Academic Press, 1972.

[2] E. Shiles, T. Sasaki, M. Inokuti, and D. Y. Smith, "Self-consistency and sum-rule tests in the Kramers–Kronig analysis of optical data: Applications to aluminum", *Phys. Rev. B*, vol. 22, pp. 1612–1628, 1980.

[3] D. Y. Smith, "Dispersion theory, sum rules, and their application to the analysis of optical data", In: *Handbook of Optical Constants of Solids (E. D. Palik, ed.)*, vol. 1, pp. 35–68, Academic Press, 1985.

[4] V. Lucarini, K.-E. Peiponen, J. J. Saarinen, and E. M. Vartiainen, *Kramers–Kronig Relations in Optical Materials Research*, Berlin: Springer, 2005.

[5] M. Dressel and G. Grüner, *Electrodynamics of Solids: Optical Properties of Electrons in Matter*, Cambridge: University Press, 2002.

[6] D. Franta, D. Nečas, and L. Zajíčková, "Application of Thomas-Reiche-Kuhn sum rule to construction of advanced dispersion models", *Thin Solid Films*, vol. 534, pp. 432–441, 2013.

[7] D. Franta, J. Vohánka, and M. Čermák, "Universal dispersion model for characterization of thin films over wide spectral range", In: *Optical Characterization of Thin Solid Films (O. Stenzel and M. Ohlídal, eds.)*, vol. 64, pp. 31–82, Springer, 2018.

[8] D. Franta, D. Nečas, L. Zajíčková, and I. Ohlídal, "Broadening of dielectric response and sum rule conservation", *Thin Solid Films*, vol. 571, pp. 496–501, 2014.

[9] D. Franta, D. Nečas, L. Zajíčková, and I. Ohlídal, "Utilization of the sum rule for construction of advanced dispersion model of crystalline silicon containing interstitial oxygen", *Thin Solid Films*, vol. 571, pp. 490–495, 2014.

[10] D. Franta, D. Nečas, L. Zajíčková, and I. Ohlídal, "Dispersion model of two-phonon absorption: application to c-Si", *Opt. Mater. Express*, vol. 4, pp. 1641–1656, 2014.

[11] D. Franta, A. Dubroka, C. Wang, A. Giglia, J. Vohánka, P. Franta, and I. Ohlídal, "Temperature-dependent dispersion model of oat zone crystalline silicon", *Appl. Surf. Sci.*, vol. 421, pp. 405–419, 2017.

[12] D. Franta, P. Franta, J. Vohánka, M. Čermák, and I. Ohlídal, "Determination of thicknesses and temperatures of crystalline silicon wafers from optical measurements in the far infrared region", *J. Appl. Phys.*, vol. 123, pp. 185707, 2018.

[13] *ISO 1:2016 – Geometrical product specifications (GPS) – Standard reference temperature for the specification of geometrical and dimensional properties.*

[14] D. Franta, D. Nečas, *et al*, *Software for optical characterization newAD2*, http://newad.physics.muni.cz.

[15] H. Ibach, "Thermal Expansion of Silicon and Zinc Oxide (I)", *Phys. Status Solidi*, vol. 31, pp. 625–634, 1969.

[16] T. Middelmann, A. Walkov, G. Bartl, and R. Schödel, "Thermal expansion coeficient of single-crystal silicon from 7 K to 293 K", *Phys. Rev. B*, vol. 92, pp. 174113, 2015.

[17] M. K. Gupta, R. Mittal, B. Singh, S. K. Mishra, D. T. Adroja, A. D. Fortes, and S. L. Chaplot, "Phonons and anomalous thermal expansion behavior of H_2O and D_2O ice Ih", *Phys. Rev. B*, vol. 98, pp. 104301, 2018.

[18] G. K. White, "Thermal expansion of reference materials: copper, silica and silicon", *J. Phys. D Appl. Phys.*, vol. 6, pp. 2070–2078, 1973.

[19] T. A. Mary, J. S. O. Evans, T. Vogt, and A. W. Sleightoddini, "Negative Thermal Expansion from 0.3 to 1050 Kelvin in ZrW_2O_8", *Science*, vol. 272, pp. 90–92, 1996.

[20] B. K. Greve, K. L. Martin, P. L. Lee, P. J. Chupas, K. W. Chapman, and A. P. Wilkinson, "Pronounced Negative Thermal Expansion from a Simple Structure: Cubic ScF_3", *J. Am. Chem. Soc.*, vol. 132, pp. 15496–15498, 2010.

[21] H. Watanabe, N. Yamada, and M. Okaji, "Linear thermal expansion coeficient of silicon from 293 to 1000 K", *Int. J. Thermophys.*, vol. 25, pp. 221–236, 2004.

[22] M. Balkanski, "Photon-phonon interactions in solids", In: *Optical properties of solids (F. Abeles, ed.)*, pp. 529–651, 1972.

[23] P. Y. Yu and M. Cardona, *Fundamentals of Semiconductors*, Springer, 2001.

[24] C. Kittel, *Introduction to Solid State Physics*, New York: Wiley, 5th ed., 1976.

[25] G. G. Macfarlane and V. Roberts, "Infrared absorption of silicon near the lattice edge", *Phys. Rev.*, vol. 98, pp. 1865–1866, 1955.

[26] D. Franta, M. Čermák, J. Vohánka, and I. Ohlídal, "Dispersion models describing interband electronic transitions combining Tauc's law and Lorentz model", *Thin Solid Films*, vol. 631, pp. 12–22, 2017.

[27] D. Campi and C. Coriasso, "Prediction of optical properties of amorphous tetrahedrally bounded materials", *J. Appl. Phys.*, vol. 64, pp. 4128–4134, 1988.

[28] G. E. Jellison, Jr. and F. A. Modine, "Parameterization of the optical functions of amorphous materials in the interband region", *Appl. Phys. Lett.*, vol. 69, pp. 371–373, 1996.

[29] G. E. Jellison, Jr. and F. A. Modine, "Erratum: Parameterization of the optical functions of amorphous materials in the interband region", *Appl. Phys. Lett.*, vol. 69, pp. 2137, 1996.

[30] A. S. Ferlauto, G. M. Ferreira, J. M. Pearce, C. R. Wronski, R. W. Collins, X. M. Deng, and G. Ganguly, "Analytical model for the optical functions of amorphous semiconductors from the near-infrared to ultraviolet: Applications in thin film photovoltaics", *J. Appl. Phys.*, vol. 92, pp. 2424–2436, 2002.

[31] D. Franta, D. Nečas, I. Ohlídal, and A. Giglia, "Dispersion model for optical thin fims applicable in wide spectral range", In: *Optical Systems Design 2015: Optical Fabrication, Testing, and Metrology V*, vol. 9628 of Proc. SPIE, pp. 96281U, 2015.

[32] D. Franta, D. Nečas, I. Ohlídal, and A. Giglia, "Optical characterization of SiO_2 thin films using universal dispersion model over wide spectral range", In: *Photonics Europe 2016: Optical Micro- and Nanometrology VI*, vol. 9890 of Proc. SPIE, pp. 989014, 2016.

[33] D. Franta, D. Nečas, A. Giglia, P. Franta, and I. Ohlídal, "Universal dispersion model for characterization of optical thin films over wide spectral range: Application to magnesium uoride", *Appl. Surf. Sci.*, vol. 421, pp. 424–429, 2017.

[34] P. B. Allen and M. Cardona, "Theory of the temperature dependence of the direct gap of germanium", *Phys. Rev. B*, vol. 23, 1981.

[35] L. Vina, S. Logothetidis, and M. Cardona, "Temperature dependence of the dielectric function of germanium", *Phys. Rev. B*, vol. 30, pp. 1979–1991, 1984.

[36] P. Lautenschlager, P. B. Allen, and M. Cardona, "Temperature dependence of band gaps in Si and Ge", *Phys. Rev. B*, vol. 31, pp. 2163–2171, 1985.

[37] P. Lautenschlager, M. Garriga, L. Vina, and M. Cardona, "Temperature dependence of the dielectric function and interband critical points in silicon", *Phys. Rev. B*, vol. 36, pp. 4821–4830, 1987.

[38] H. L. Smith, Y. Shen, D. S. Kim, F. C. Yang, C. P. Adams, C. W. Li, D. L. Abernathy, M. B. Stone, and B. Fultz, "Temperature dependence of phonons in $FeGe_2$", *Phys. Rev. Mater.*, vol. 2, pp. 103602, 2018.

[39] C. Keffer, T. M. Hayes, and A. Bienenstock, "PbTe Debye-Waller factors and band-gap temperature dependence", *Phys. Rev. Lett.*, vol. 21, pp. 1676–1678, 1968.

[40] H. Haas, C. Z. Wang, K. M. Ho, M. Fähnle, and C. Elsässer, "Temperature dependence of the phonon frequencies of molybdenum: a tightbinding molecular dynamics study", *J. Phys. Con-des. Matter*, vol. 11, pp. 5455–5462, 1999.

[41] B. J. Frey, D. B. Leviton, and T. J. Madison, "Temperature-dependent refractive index of silicon and germanium", In: *Optomechanical Technologies for Astronomy*, vol. 6237 of Proc. SPIE, pp. 62732J, 2006.

Received 19 March 2019